


 Cite this: *Chem. Commun.*, 2023, 59, 9599

 Received 28th April 2023,
 Accepted 10th July 2023

DOI: 10.1039/d3cc02076b

rsc.li/chemcomm

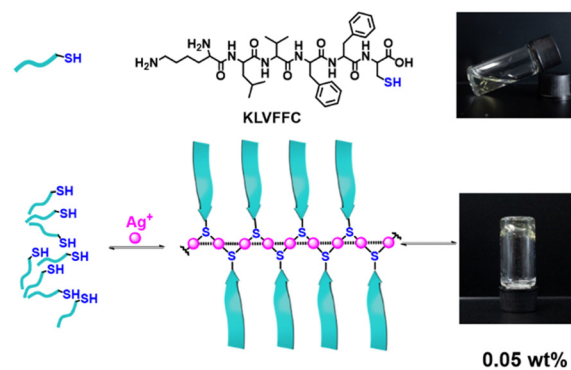
Amyloid peptide hydrogels *via* formation of coordination polymers with Ag⁺ by its core peptide equipped with a C-cysteine†

 Qian Wang,^{ib*} Fu-Peng Zhou, Dan-Dan Tao, Jin-Hong Wei, Rui Cai and Yun-Bao Jiang^{ib*}

We report that the core sequence of amyloid β (Aβ) peptide, KLVFF, when equipped with a C-terminal cysteine residue, exhibited an extremely low minimum hydrogelation concentration of 0.05 wt% in the presence of Ag⁺ in pH 5 buffer, with this concentration 2 orders of magnitude lower than that of the pentapeptide itself. The CD signal of the Ag⁺-L-KLVFFC hydrogel was observed to be sensitive to the early-stage aggregation of amyloid β peptide.

As soft materials, peptide-based hydrogels have attracted remarkable attention because of their intrinsic biocompatibility and biodegradability, and have been utilized as platforms for chem/biosensing, tissue engineering, drug delivery, and wound healing.^{1–3} The generation of peptide-based hydrogels relies on a hierarchical assembly of peptides into nanostructures *via* a variety of supramolecular interactions such as hydrogen bonding, aromatic interactions, hydrophobic interactions, and electrostatic interactions.⁴ Particularly, peptides that adopt a β-sheet secondary structure have been widely employed to create hydrogels.^{5–7} The Alzheimer's-disease-implicated amyloid β (Aβ) peptide is one of the most well-known peptides that form β-sheet-rich fibril structures upon self-assembling. The key motif pentapeptide Aβ(16–20), *i.e.*, KLVFF, has been reported to be crucial for amyloid fibrillization.⁸ On the basis of the KLVFF sequence, many hydrogelators have been developed with excellent mechanical properties and low minimum gelling concentrations.⁹ Although KLVFF peptide self-assembles into a β-sheet-rich fibre structure, it remains liquid in water up to a concentration of 4 wt%, while fragile hydrogels form only in PBS solutions at 3 wt% because of the enhanced electrostatic interactions between their side chains.¹⁰

Our group previously reported cysteine and cysteine-derived ligands, in the presence of Ag⁺, forming coordination polymers and hydrogels in aqueous solutions; the formation of these products was substantially facilitated by the argentophilic interactions (Ag⁺···Ag⁺ interactions) along the backbone and the interactions between side chains of the ligands attached to the backbone.^{11–15} We thus envisaged that the gelation of the Aβ core peptide sequence would be enhanced when equipped with a terminal cysteine residue (Scheme 1). We specifically envisaged that, in the presence of Ag⁺, the formation of Ag⁺-peptide coordination polymers would promote the directional assembly of the peptides along the polymeric backbone by bringing the peptide molecules close together, hence yielding a higher local concentration, stronger interactions, and consequently enhanced gelation. Herein we report our discovery of the indeed dramatically enhanced hydrogelation of the KLVFF sequence equipped with a C-terminal cysteine residue, in the presence of Ag⁺ in a buffer of pH 5, with an extremely low minimum gelation concentration of 0.05 wt%, *ca.* 2 orders of magnitude lower that of the pentapeptide itself.



Scheme 1 Structure of KLVFFC (KC) and schematic depiction of interactions between KC and Ag⁺ in the formed coordination polymer and hydrogel.

Department of Chemistry, College of Chemistry and Chemical Engineering, The MOE Key Laboratory of Spectrochemical Analysis and Instrumentation, and iChEM, Xiamen University, Xiamen 361005, China. E-mail: ybjiang@xmu.edu.cn

† Electronic supplementary information (ESI) available. See DOI: <https://doi.org/10.1039/d3cc02076b>

Hexapeptide *L*- or *D*-**KLVFFC** (**KC**, Scheme 1) was dissolved in 0.1 M HNO₃ followed by heating to make sure that the peptide became fully disaggregated. The final pH of the solution was adjusted to 5 using aqueous NH₃. Hydrogels were formed instantly upon adding 1 equivalent of Ag⁺ to the peptide solution, by specifically using a 0.1 M AgNO₃ stock solution, and remained stable for several days. The minimum gelling concentration of *L*-**KC** and *D*-**KC** peptides in the presence of Ag⁺ was found to be 0.05 wt% (0.66 mM), whereas the peptide itself remained in solution, but did precipitate in the absence of Ag⁺ (Scheme 1). For comparison, Ag⁺-*rac*-**KC** hydrogels were also prepared by adding Ag⁺ to the enantiomeric mixture of *L*-**KC** and *D*-**KC**, with the minimum gelling concentration of the opaque hydrogel being much higher than 0.5 wt%. The self-supporting nature of the gels was evident upon inverting a vial containing a sample of the gel (Fig. S1, ESI†). The *L*-**KLVFF** peptide hydrogel was prepared using the above-mentioned method, but no gel formation was observed at 1.0 wt% (Fig. S2, ESI†).

Absorption and circular dichroism (CD) spectra of *L*-**KC** and *D*-**KC** peptides in the presence of Ag⁺ of increasing concentration were first examined, in order to demonstrate the formation of Ag⁺-*L*-**KC** and Ag⁺-*D*-**KC** coordination polymers and their supramolecular chirality. *L*-**KC** peptide, for example, in aqueous solution showed a negative Cotton effect at a wavelength of 191 nm and a weak positive Cotton effect at 220 nm, indicating the random coil nature of the secondary structure of the free peptide.¹⁶ In the presence of Ag⁺, a new band at 345 nm developed in both absorption and CD spectra (Fig. 1b and d), a sign of the occurrence of Ag⁺...Ag⁺ interactions,¹⁷ which suggested the formation of Ag⁺-**KC** coordination polymers. Mirror-image-related CD signals at 283 nm and 345 nm were observed for *D*-**KC** in the presence of Ag⁺, suggesting that the supramolecular chirality of the Ag⁺-*L*-**KC** and Ag⁺-*D*-**KC** coordination polymers was due to the molecular chirality of the **KC** peptide. Plots of absorbance and CD signal against concentration of Ag⁺ showed a 1:1 stoichiometry (Fig. S3 and S4, ESI†). Increasing the concentration of Ag⁺-*L*-**KC** or Ag⁺-*D*-**KC**

coordination polymers, up to 0.05 wt%, led to the formation of hydrogels, with concomitant increases in the intensities of the absorbance and CD signals but no changes in their spectral profiles (Fig. S5 and S6, ESI†). This result indicated that gelation did not change the supramolecular chirality of the Ag⁺-**KC** coordination polymers.

The ¹H NMR spectra of *L*-**KC** and *D*-**KC** showed well-resolved signals; significantly broader signals were observed in the spectra of the Ag⁺-*L*-**KC** and Ag⁺-*D*-**KC** hydrogel samples (Fig. S20, ESI†), indicating formation of the coordination polymers. The MALDI-TOF mass spectra of the Ag⁺-*L*-**KC** and Ag⁺-*D*-**KC** hydrogels suggested the presence of several types of repeat units composed of dimeric **KC** peptides and Ag⁺ (Fig. S21, ESI†). FT-IR and XRD measurements were also taken to elucidate the gelation mechanism in terms of the peptide secondary structure (Fig. 2a and b). In general, the amide I region IR (1600–1700 cm⁻¹), assigned to the stretching of amide C=O in the peptide backbone, is a useful tool to analyse peptide secondary structures; for example, bands at 1610–1640 cm⁻¹ and about 1700 cm⁻¹ are assigned to anti-parallel β-sheet structures.¹⁸ Compared to the **KC** peptide, the Ag⁺-*L*-**KC** or Ag⁺-*D*-**KC** hydrogel in the current work showed a strong band at 1637 cm⁻¹ and a weaker broad band at about 1685 cm⁻¹, suggesting an anti-parallel-β-sheet packing of the peptide backbones in the hydrogel framework. A new band appeared at 1725 cm⁻¹ upon hydrogelation, likely resulting from stretching of COOH in the side chains of the ligands,^{19,20} which suggested possible hydrogen bonding between side chains in the hydrogel. CD spectra of the coordination polymers in the sol state examined as a function of the enantiomeric excess (ee) of **KC** showed a linear CD-ee dependence (Fig. S8, ESI†). This result indicated a self-sorting of the ligands upon formation of their coordination polymers of Ag⁺ and indicated a highly ordered structure of the peptide chain, despite its intrinsic flexibility, when attached to the polymeric backbone. The FT-IR and CD

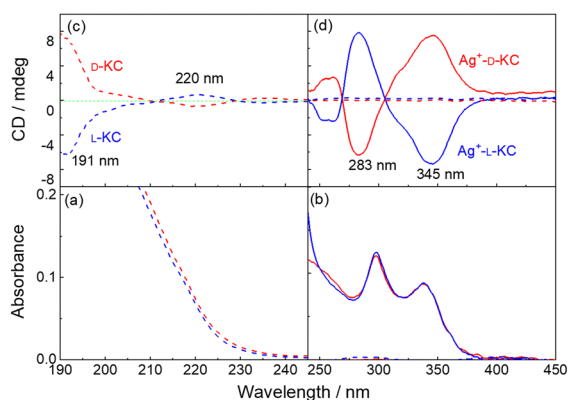


Fig. 1 Absorption (a), (b) and CD (c), (d) spectra of *L*-**KC** and *D*-**KC** peptides (dashed lines) and Ag⁺-*L*-**KC** and Ag⁺-*D*-**KC** coordination polymers (solid lines), measured in 1 mm cuvettes. [Ag⁺] = [*L*-**KC**] = [*D*-**KC**] = 100 μM or 0.0076 wt%.

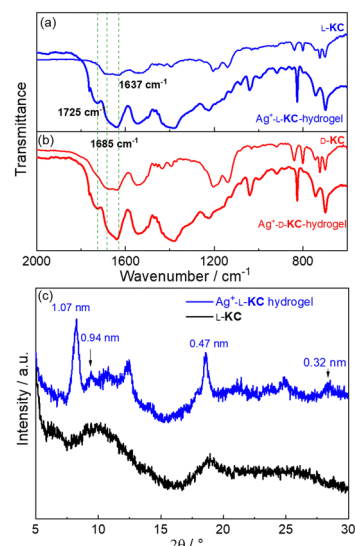


Fig. 2 FT-IR spectra (a), (b) and XRD patterns (c) of *L*-**KC** and *D*-**KC** and hydrogels of Ag⁺-*L*-**KC** and Ag⁺-*D*-**KC**.

spectral data thus indicated that the coordination of Ag^+ to **KC** peptide promoted a secondary structural transformation of the peptide from random coil to β -sheet, favourable for the interactions between side chains of the ligands in the coordination polymers and in turn the hydrogelation of the peptides. X-ray diffraction (XRD, Fig. 2c) of lyophilized Ag^+ -**L-KC** hydrogels showed peaks corresponding to 0.94 nm, 0.47 nm and 0.32 nm, corresponding to ratios of 1, 1/2 and 1/3, respectively. This result indicated a lamellar structure for the hydrogel, with a *d*-spacing of 0.94 nm, calculated using the Bragg equation.²¹

Morphologies of **L-KC** and **D-KC** peptides and their assembled structures, *i.e.*, Ag^+ -**KC** coordination polymers, were characterized using TEM and SEM. Peptides **L-KC** and **D-KC** formed fibre-like structures, with widths of *ca.* 10 nm (Fig. 3a and b). Self-assembled **L-KLVFF** peptide also showed fibre-like structures that corresponded well with the cryo-TEM results in the literature (Fig. S2, ESI[†]).¹⁰ The dried samples of Ag^+ -**L-KC** and Ag^+ -**D-KC** coordination polymers in the sol state already showed a lamellar morphology (Fig. 3c and d), agreeing with the conclusion of strong crosslinking and packing of **KC** peptides in the β -sheet structure upon binding Ag^+ , as also indicated in the XRD pattern (Fig. 2c). Lyophilized Ag^+ -**L-KC** and Ag^+ -**D-KC** hydrogels showed each a relatively compact lamellar morphology (Fig. 3e and f). Mechanical properties of Ag^+ -**KC** hydrogels were investigated by performing rheometry, using a parallel plates geometry with 20 mm plates and a sample thickness of 500 microns. The linear viscoelastic region (LVR) of the stress-strain response was determined using amplitude sweep over the region of 0.1%–100%. Dynamic shear amplitude sweeps at 10 rad s^{-1} showed gel breaking under strain from 10% to 50% (Fig. S9 and S10, ESI[†]). For time and frequency sweep measurements, LVR of 1% was used for 0.05 wt%

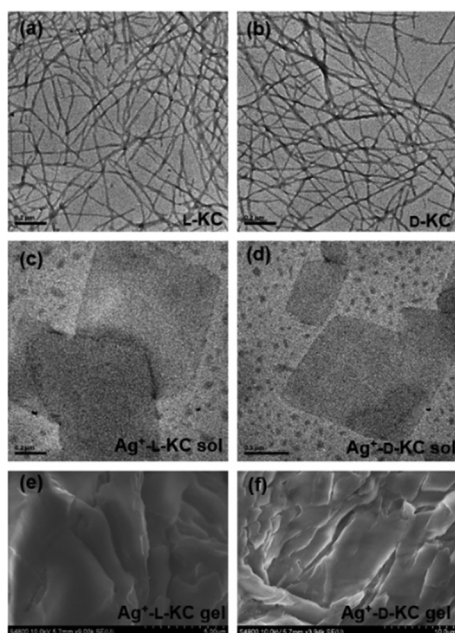


Fig. 3 TEM images of **L-KC** (a), **D-KC** (b), Ag^+ -**L-KC** (c) and Ag^+ -**D-KC** (d) and SEM images of lyophilized Ag^+ -**L-KC** (e) and Ag^+ -**D-KC** (f) hydrogels.

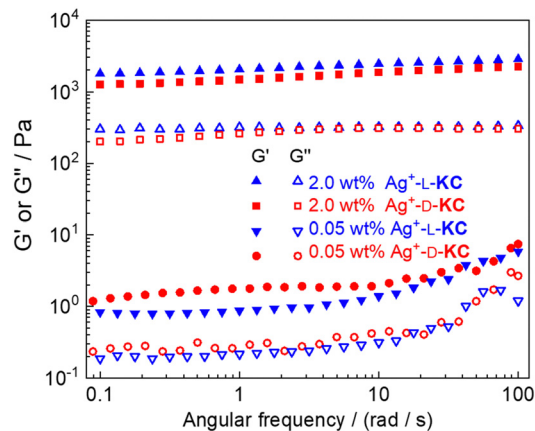


Fig. 4 Rheological properties of Ag^+ -**L-KC** and Ag^+ -**D-KC** hydrogels at the minimum hydrogelation concentration of 0.05 wt% and at 2.0 wt%, examined at 1% and 3% strains, respectively.

hydrogels and LVR of 3% was used for 2.0 wt% hydrogels. For 0.05 wt% Ag^+ -**L-KC** and Ag^+ -**D-KC** hydrogels, the storage modulus G' was *ca.* 1 order of magnitude larger than the loss modulus G'' , indicating the gel nature of the materials (Fig. 4). For 2.0 wt% Ag^+ -**L-KC** and Ag^+ -**D-KC** hydrogels, the high G' values suggested that the hydrogels exhibited good mechanical properties (Fig. 4). The mechanical character of the 2.0 wt% Ag^+ -**rac-KC** hydrogel was also assessed (Fig. S11, ESI[†]), and its storage modulus was measured to be significantly lower than those of Ag^+ -**L-KC** or Ag^+ -**D-KC** hydrogels, possibly due to the high tendency for the peptide to precipitate in the racemic hydrogel.

Finally, the Ag^+ -**KC** hydrogels were applied for sensing of $\text{A}\beta(1-40)$ monomer and aggregates. $\text{A}\beta(1-40)$ peptide was disaggregated and prepared according to an established protocol.²² $\text{A}\beta(1-40)$ monomer film was suspended in DMSO to a concentration of 2.5 mM, followed by being subjected to vortex sonication, and then being diluted with PBS buffer (pH 7.5) to a final concentration of 50 μM and incubated at 37 $^{\circ}\text{C}$ to allow for it to aggregate. Samples of $\text{A}\beta(1-40)$ monomer of increasing concentration and oligomers, respectively, were mixed with samples of **L-KC** or **D-KC** peptide prior to the addition of Ag^+ , after which the CD signals of the resulting hydrogels were measured. For the Ag^+ -**D-KC** hydrogel and even to a higher extent for the Ag^+ -**L-KC** hydrogel, the CD signal at 345 nm was found to be quenched by $\text{A}\beta(1-40)$ monomer (Fig. 5a). The results also suggested that the $\text{Ag}^+ \cdots \text{Ag}^+$ interactions were increasingly weakened by increasing concentrations of $\text{A}\beta(1-40)$ monomer (Fig. S12–S14, ESI[†]). Based on these results, the supramolecular chirality was concluded to have been perturbed by $\text{A}\beta$ monomers. Surprisingly, substantial quenching by up to 70% of the CD signal of the Ag^+ -**L-KC** hydrogel by $\text{A}\beta(1-40)$ aggregates was observed after incubation for 6 h, whereas that of the Ag^+ -**D-KC** hydrogel underwent almost no change, again exhibiting an enantiomeric discrimination (Fig. 5b and Fig. S15–S17, ESI[†]). As the incubation time was increased from 6 to 12 h, the CD signal was quenched to decreasing extents, indicating a lack of effect of larger aggregations of $\text{A}\beta(1-40)$ on the $\text{Ag}^+ \cdots \text{Ag}^+$ interactions in the hydrogel

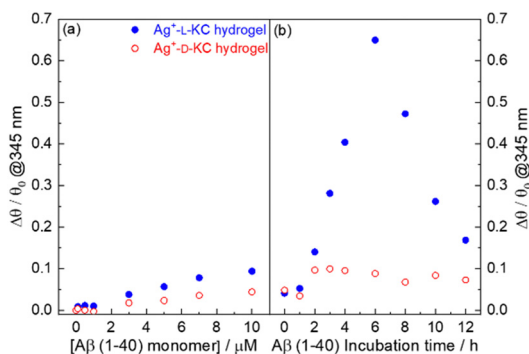


Fig. 5 Quenching of CD at 345 nm of Ag⁺-L-KC and Ag⁺-D-KC hydrogels by Aβ(1-40) monomer (a) and Aβ(1-40) aggregates (b). Concentration of hydrogels was maintained at 0.1 wt%. [Aβ(1-40) monomer] = 0.1–10 μM; for aggregation assay [Aβ(1-40) aggregates] = 1 μM.

network. Aggregation of Aβ(1-40) was at the same time monitored using the classic thioflavin T (ThT) fluorescence assay, which showed that during the initial stage of incubation, from 0–10 h, Aβ(1-40) peptide was at the nucleation phase (Fig. S18 and S19, ESI[†]).²³ This observation was of great significance for the observed substantial change in the CD signal of Ag⁺-L-KC hydrogels for sensing early-stage Aβ aggregation, because conventional spectroscopic methods for studying Aβ aggregation usually lack sensitivity to the initial nucleation phase,²⁴ a critical stage in the development of Alzheimer's disease.^{25,26} Our results, therefore, showed that the Ag⁺-KC hydrogels could be powerful label-free materials for sensing and probing Aβ peptides at their early aggregation stage. Note that HeLa cells showed high viability in the presence of low concentrations of Ag⁺-L-KC, but their viability decreased as the concentration of Ag⁺-L-KC was increased from 0.025 wt% to 0.05 wt% (Fig. S22, ESI[†]).

In summary, we proposed and verified a scheme to enhance the hydrogelation of short peptides by taking the core pentapeptide in Aβ(1-40), **KLVFF**, as an example, and equipping it with a C-terminal cysteine residue to form the hexapeptide **KLVFFC** (L/D-KC). This hexapeptide, in the presence of Ag⁺, exhibited an extremely low gelation concentration of 0.05 wt% in pH 5 buffer, almost 2 orders of magnitude lower than that of the pentapeptide itself. This result was rationalized by the formation of Ag⁺-KC coordination polymers that brought the peptides in the polymeric backbone into close proximity and thereby enhanced interactions and gelation. Indeed, a characteristic anti-parallel-β-sheet packing pattern was found to be present in the Ag⁺-KC hydrogels, and these hydrogels were found to be structurally similar to the semiflexible biopolymers.²⁷ Notably, CD signals of the Ag⁺-L-KC hydrogels, but not the Ag⁺-D-KC hydrogels, were shown to be sensitive to the early-stage aggregation of Aβ(1-40), being therefore a powerful label-free material for identifying Aβ at its early aggregation stage. We expect that this strategy of enhancing gelation of peptides, by attaching a terminal cysteine residue to allow formation of coordination polymers with Ag⁺, will prove applicable to a broad range of functional peptides, for eventually making peptide-based soft materials.

We are thankful for the support provided by the National Science Foundation of China (grants 21820102006, 91856118, 21904111 and 22241503) and by the Ministry of Education of China *via* fundamental research funds for the central universities (grants 20720220005 and 20720220121). We thank Professor Tao Jiang of Xiamen University for all cell culture and cytotoxicity experiments.

Conflicts of interest

There are no conflicts to declare.

Notes and references

- X. Du, J. Zhou, J. Shi and B. Xu, *Chem. Rev.*, 2015, **115**, 13165–13307.
- T. Guan, J. Li, C. Chen and Y. Liu, *Adv. Sci.*, 2022, **9**, 2104165.
- Z. Zhang, S. Ai, Z. Yang and X. Li, *Adv. Drug Delivery Rev.*, 2021, **174**, 482–503.
- J. Li and D. J. Mooney, *Nat. Rev. Mater.*, 2016, **1**, 16071.
- D. E. Clarke, C. D. J. Parmenter and O. A. Scherman, *Angew. Chem., Int. Ed.*, 2018, **57**, 7709–7713.
- S. Das, R. Kumar, N. N. Jha and S. K. Maji, *Adv. Healthcare Mater.*, 2017, **6**, 1700368.
- B. Hu, Y. Shen, J. Adamcik, P. Fischer, M. Schneider, M. J. Loessner and R. Mezzenga, *ACS Nano*, 2018, **12**, 3385–3396.
- I. W. Hamley, *Chem. Rev.*, 2012, **112**, 5147–5192.
- A. Dasgupta, J. H. Mondal and D. Das, *RSC Adv.*, 2013, **3**, 9117–9149.
- M. J. Krysmann, V. Castelletto, A. Kellarakis, I. W. Hamley, R. A. Hule and D. J. Pochan, *Biochemistry*, 2008, **47**, 4597–4605.
- D.-H. Li, J.-S. Shen, N. Chen, Y.-B. Ruan and Y.-B. Jiang, *Chem. Commun.*, 2011, **47**, 5900–5902.
- J.-S. Shen, D.-H. Li, M.-B. Zhang, J. Zhou, H. Zhang and Y.-B. Jiang, *Langmuir*, 2011, **27**, 481–486.
- Q. Zhang, Y. Hong, N. Chen, D.-D. Tao, Z. Li and Y.-B. Jiang, *Chem. Commun.*, 2015, **51**, 8017–8019.
- J.-S. Shen, L.-H. Dong, C.-G. Qing and Y.-B. Jiang, *J. Mater. Chem.*, 2009, **19**, 6219–6224.
- Q. Zhang, Q. Wang, X.-X. Chen, P. Zhang, C.-F. Ding, Z. Li and Y.-B. Jiang, *Trends Anal. Chem.*, 2018, **109**, 32–42.
- I. Gokce, R. W. Woody, G. Anderlueh and J. H. Lakey, *J. Am. Chem. Soc.*, 2005, **127**, 9700–9701.
- Q. Wang, S.-L. Dong, D.-D. Tao, Z. Li and Y.-B. Jiang, *Coord. Chem. Rev.*, 2021, **432**, 213717.
- J. Seo, W. Hoffmann, S. Warnke, X. Huang, S. Gewinner, W. Schöllkopf, M. T. Bowers, G. von Helden and K. Pagel, *Nat. Chem.*, 2017, **9**, 39–44.
- A. Barth, *Biochim. Biophys. Acta*, 2007, **1767**, 1073–1101.
- B. Nie, J. Stutzman and A. Xie, *Biophys. J.*, 2005, **88**, 2833–2847.
- L. Yang, F. Wang, D.-I. Y. Auphedeous and C. Feng, *Nanoscale*, 2019, **11**, 14210–14215.
- W. B. Stine, K. N. Dahlgren, G. A. Krafft and M. J. LaDu, *J. Biol. Chem.*, 2003, **278**, 11612–11622.
- D. Shea, C.-C. Hsu, T. M. Bi, N. Paranjapye, M. C. Childers, J. Cochran, C. P. Tomberlin, L. Wang, D. Paris, J. Zonderman, G. Varani, C. D. Link, M. Mullan and V. Daggett, *Proc. Natl. Acad. Sci. U. S. A.*, 2019, **116**, 8895–8900.
- K. L. Viola, J. Sbarboro, R. Sureka, M. De, M. A. Bicca, J. Wang, S. Vasavada, S. Satpathy, S. Wu, H. Joshi, P. T. Velasco, K. MacRenaris, E. A. Waters, C. Lu, J. Phan, P. Lacor, P. Prasad, V. P. Dravid and W. L. Klein, *Nat. Nanotech.*, 2015, **10**, 91–98.
- I. Benilova, E. Karran and B. D. Stroope, *Nat. Neurosci.*, 2012, **15**, 349–357.
- T. Kondo, M. Asai, K. Tsukita, Y. Kutoku, Y. Ohsawa, Y. Sunada, K. Imamura, N. Egawa, N. Yahata, K. Okita, K. Takahashi, I. Asaka, T. Ao, A. Watanabe, K. Watanabe, C. Kadoya, R. Nakano, D. Watanabe and H. Inoue, *Cell Stem Cell*, 2013, **12**, 487–496.
- B. Sarkar, Z. Siddiqui, P. K. Nguyen, N. Dube, W.-Y. Fu, S. Park, S. Jaisinghani, R. Paul, S. D. Kozuch, D.-Y. Deng, P. I. Montoro, M.-Y. Li, D. Sabatino, D. S. Perlin, W. Zhang, J. Mondal and V. A. Kumar, *ACS Biomater. Sci. Eng.*, 2019, **5**, 4657–4670.